

Instance-wise Linearization of Neural Network for Model Interpretation

Zhimin Li

University of Utah

zhimin@sci.utah.edu

Shusen Liu

Lawrence Livermore National Laboratory

liu42@llnl.gov

Kailkhura Bhavya

Lawrence Livermore National Laboratory

kailkhura1@llnl.gov

Timo Bremer

Lawrence Livermore National Laboratory

bremer5@llnl.gov

Valerio Pascucci

University of Utah

pascucci@sci.utah.edu

Abstract

Neural network have achieved remarkable successes in many scientific fields. However, the interpretability of the neural network model is still a major bottlenecks to deploy such technique into our daily life. The challenge can dive into the non-linear behavior of the neural network, which rises a critical question that how a model use input feature to make a decision. The classical approach to address this challenge is feature attribution, which assigns an important score to each input feature and reveal its importance of current prediction. However, current feature attribution approaches often indicate the importance of each input feature without detail of how they are actually processed by a model internally. These attribution approaches often raise a concern that whether they highlight correct features for a model prediction.

For a neural network model, the non-linear behavior is often caused by non-linear activation units of a model. However, the computation behavior of a prediction from a neural network model is locally linear, because one prediction has only one activation pattern. Base on the observation, we propose an instance-wise linearization approach to reformulates the forward computation process of a neural network prediction. This approach reformulates different layers of convolution neural networks into linear matrix multiplication. Aggregating all layers' computation, a prediction complex convolution neural network operations can be described as a linear matrix multiplication $F(x) = W \cdot x + b$. This equation can not only provides a feature attribution map that highlights the important of the input features but also tells how each input feature contributes to a prediction exactly. Furthermore, we discuss the

application of this technique in both supervise classification and unsupervised neural network learning parametric t-SNE dimension reduction.

1. Introduction

Neural network techniques have achieved remarkable success across many scientific fields [13, 26, 30, 6]. Furthermore, many applications (e.g., autopilot, debt loan, cancer detection, criminal justice,...) which utilize this technology, starts to involve into our daily life and even more in the expected future. However, the uninterpretable behavior of the neural network prediction causes many concerns. For example, recently, a few countries' governments have published AI act [1, 38] to regulate AI systems and require automate systems must provide an explanation for why it makes such a decision. Meanwhile, improving the interpretability of the neural network can also benefit scientific fields for knowledge discover, such as drug discover [36, 2]

A key challenge of the neural network interpretability is the non-linear behavior of the neural network model. These non-linear behaviors are caused by different activation patterns which are triggered by different inputs, and these diverse activation patterns lead to an uninterpretable behavior. A classical approach to explain neural network prediction is the feature attribution method [16, 22], which assigns an important score to each input feature and highlight the most important features. However, different feature attribution approaches may end up with different feature maps, and how input features are processed by the neural network model internally is mysterious [41].

For a single neural network prediction, the neural network model has only single activation pattern. The input

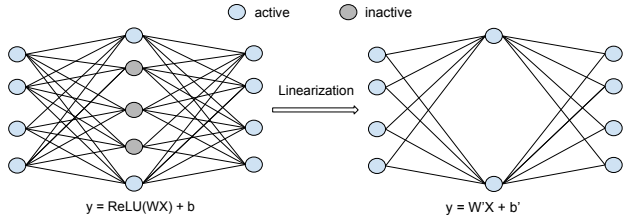


Figure 1. A prediction of neural network model has only one activation pattern and the complex prediction operation can be simplified as a linear matrix multiplication.

features which are processed by the neural network layer by layer during the prediction is linear. It raises a question that whether the computation process of a neural network can generate an answer of how each input feature contributes to the prediction. In this study, we propose an approach to reformulate the decision process of a neural network prediction and reformulate the forward computation process of a neural network prediction. Our approach is based on an observation that a neural network prediction has only one activation pattern. As the Figure 1 shows, the non-linear ReLU activation components of a neural network prediction can be consider as linear components. Therefore, the non-linear matrix multiplication of a neural network performs on a single prediction is linear process. The whole computation process can be reformulated and aggregated into a linear equation $F(x) = W \cdot x + b$.

We find that this linear equation can be used to explain how the input feature is used by the neural network model to make prediction. In this paper, we discuss how to reformulate the forward propagation of a neural network layer by layer and discuss the potential challenge of this computation. We propose an efficient approach to calculate W^* , b^* , and discuss the role of W^* and b^* during model prediction. Our approach is much more flexible and can be applied to supervise learning task or unsupervised learning task.

At the end, we demonstrate a use case of how neural network models capture input feature in different layer of network models and how researchers can use our technique to understand the behavior of neural network models.

2. Relative Work

Because of the black-box nature of the neural network model, understanding how it makes prediction is an important but challenge topic. In this section, we discuss previous techniques that have been proposed in the literature to address this challenge.

2.1. Feature Attribution

Feature attribution is a classical approach, which generates a heat map to highlight the importance of input feature for a model prediction. Different methodology has

been designed to calculate the heat map. Gradient base approaches [31, 34, 25, 33] calculate the model gradient of an input with respect to the target label and use or accumulate the gradient values to highlight the importance of each input feature. Perturbation base approaches [20, 7, 8, 39, 22] ablate or modify a part of the input and observe the output variation to understand the contribution of each input feature to the prediction. Other approach like SHAP [16], Deep-Lift [29], and LRP [3] provide a feature attribution map from different angle. However, because of the lacking of ground truth, whether a feature attribution approach highlights the real important regions of an input is still under exploration.

Understanding features that captured by a neuron of neural network can also improve the interpretability of neural network. Feature visualization [19] optimizes an input image by maximizing a neuron’s activation value. The output of the optimization provides information about what features are captured by the neuron. Previous researchers [4, 40] have also measured the alignment between individual neuron unit and semantic concepts. Fong et al. [7] applies input perturbation to measure the reaction of a neuron to these perturbation and capture the input regions that contribute most to these activation.

2.2. Local Linearity of Neural Network

Researchers have investigated the local linearity of ReLU network, which mainly focus on the complexity of the model such as approximating the number of linear regions [23, 28, 9, 17, 21, 27]. Previous researches have also aligned local linearity with input perturbation to understand a model’s prediction robustness and generalization. Novak, et al [18] performs a large scale experiments on different neural network models to show that input-output Jacobian norm of samples is correlated with model generalization. Lee, et al. [15] design algorithm to expand the local linear region of neural network model.

3. Instance-wise Linearization

In this section, we discuss how to transform different layers of neural network into linear operation under this condition. After transforming all layers, we demonstrate how to aggregate all linear operations into a linear matrix multiplication (1). In this study, we mainly focus our discussion on convolution neural network, which is the de-facto setting for many computer vision tasks.

$$F(x) = W \cdot x + b \quad (1)$$

A series operations of a neural network can be represented as a nest function $F(x) = f_n \cdot f_{n-1} \dots f_2 \cdot f_1$ and n is the number of layers in neural network. The detail operation of each layer can be generalized as $f_i = \sigma(W_i \cdot x_i + b_i)$.

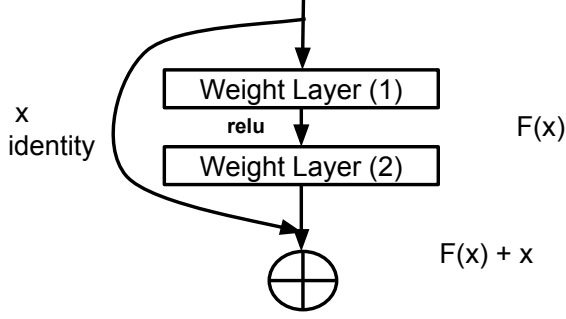


Figure 4. A skip connection component in ResNet architecture.

3.4. Skip Connection

Skip connection is a critical component in the ResNet [10] architecture. In Fig. 4 is an example of the skip connection and the equation can be representation as $F(x) + x$. In the equation, $F(x)$ is often consisted of convolution layer, batch normalization, ReLU activation and Full connected layers. As we discuss in previous section, these layers can be simplified as a linear matrix multiplication $F(x) = W_{skip} \cdot x + b_{skip}$. The overall equation can be rephrase as

$$(W_{skip} + I) \cdot x + b_{skip}$$

Merging the identify matrix I into W_{skip} and the equation can be simplified into $W'_{skip} \cdot x + b_{skip}$.

3.5. Batch Normalization Layer

Batch normalization [12] is a critical component in neural network model which makes the training easy and efficient. The inference process of the batch normalization layer is an element-wise linear transformation in equation 3. The equation that used to perform batch normalization on a single value is described as following:

$$y = \frac{x_i - \mu}{\sqrt{\sigma^2 + \epsilon}} * \gamma + \beta = \frac{\gamma}{\sqrt{\sigma^2 + \epsilon}} * x_i + \frac{-\mu\gamma}{\sqrt{\sigma^2 + \epsilon}} + \beta \quad (3)$$

In the equation, μ , σ^2 , γ , and β are calculated during the training process. These variables are available during the network inference. This equation can be rephrased as $y = w_i^{norm} * x_i + b_i^{norm}$ and $w_i^{norm} = \frac{\gamma}{\sqrt{\sigma^2 + \epsilon}}$, $b_i^{norm} = \frac{-\mu\gamma}{\sqrt{\sigma^2 + \epsilon}} + \beta$. The batch layer operation can be represented as:

$$W^{norm} \odot x + b$$

3.6. Layer Aggregation

We have mentioned that a neural network can be defined as a nest function $F(x) = f_n \cdot f_{n-1} \dots f_2 \cdot f_1$ and each layer's function can be generalized as following:

$$f_i = \sigma(W_i \cdot x_i + b_i)$$

With our previous description, for a single prediction, each layer can be replaced as a linear matrix multiplication

$$f_i = W'_i \cdot x_i + b'_i$$

and the overall equation can be rephrased as

$$F(x) = W'_n \cdot W'_{n-1} \dots W'_2 \cdot W'_1 \cdot x + \sum_{i=1}^{n-1} (W'_n \dots W'_{i+1} \cdot b_i) + b_n$$

After linearization of a neural network prediction, the prediction is represented as $F(x) = W \cdot x + b$. In the equation, $W = W'_n \cdot W'_{n-1} \dots W'_2 \cdot W'_1$ and $b = \sum_{i=1}^{n-1} (W'_n \dots W'_{i+1} \cdot b_i) + b_n$. For piece-wise linear activation function, the inference behavior of neural network model is locally linear. In a local region, the behavior of neural network on input x is equal to $F(x) = W \cdot x + b$.

Lemma 1 For a network with piece-wise linear activation function, for $x \in R^m$, there is a maximum $|\delta| \in R^m$ such that $\forall \theta, |\theta| < |\delta|$ and $x + \theta$ has the same activation pattern as x . The matrix W can be used to explain the prediction of $x + \theta$ and x .

Under this condition, the feature attribution W is equal to input-output Jacobian matrix $J_F(x)$, and W not only tells the sensitivity of input with respect to the model prediction but also represents how neural network use input to make prediction exactly. ReLU networks split the input space into linear regions [17]. In each linear region, these samples share the same explainable matrix W .

$$J_F(x) = \left[\frac{\partial F(x)_1}{\partial x}, \frac{\partial F(x)_2}{\partial x}, \dots, \frac{\partial F(x)_n}{\partial x} \right]^T = W$$

For piece-wise linear activation function, a prediction of neural network has an equivalent input and output linear mapping $y = W \cdot x + b$. However, activation function such as GELU, SELU and ELU can not use Jacobian matrix to calculate W . Therefore, the equation for $y = W \cdot x + b$ need to be calculated layer by layer.

3.7. Ensemble Model

A prediction of ensemble neural network model can be represented as

$$F(x) = \sum_{i=1}^n a_i F_i(X)$$

F_i is the individual neural network and the a_i is the share assigned to the prediction of the i_{th} neural network. As we discuss in section 3.8, the equation can be rephrased as

$$F(x) = \sum_{i=1}^n a_i (W_i^* \cdot x + b_i^*) = \left(\sum_{i=1}^n a_i W_i^* \right) \cdot x + \sum_{i=1}^n a_i b_i^*$$

Network	$W \cdot x$	b_{LFR}	b	Accuracy
Lenet300	0.9794	0.8161	0.1828	0.982
Lenet5	0.9927	0.8408	0.1596	0.9924

Table 1. Compare the prediction accuracy and label flip rate of $W \cdot x$ and b with original accuracy of MNIST test dataset over LeNet5 and LeNet300 model.

Network	$W \cdot x$	b_{LFR}	b	Accuracy
LeNet5	0.3672	0.6222	0.3307	0.754
AlexNet	0.305	0.3416	0.6223	0.8468
VGG16	0.3782	0.1116	0.8567	0.9123
VGG19	0.4257	0.1129	0.8544	0.9113
ResNet18	0.1817	0.0976	0.8756	0.9219
ResNet50	0.2496	0.1093	0.8687	0.9217
ResNet152	0.2398	0.0965	0.8758	0.927
DenseNet121	0.1957	0.0893	0.8876	0.9328

Table 2. Compare the prediction accuracy and label flip rate of $W \cdot x$ and b with original accuracy of cifar10 test dataset over different CNN architectures.

Network	$W \cdot x$	b_{LFR}	b	Accuracy
AlexNet	0.0487	0.6504	0.3061	0.6108
VGG16	0.0471	0.3559	0.5918	0.7254
VGG19	0.0397	0.3297	0.6073	0.7176
ResNet18	0.1344	0.355	0.5931	0.7636
ResNet50	0.1581	0.3164	0.633	0.7911
ResNet101	0.1388	0.2854	0.6624	0.7961
ResNet152	0.1545	0.2898	0.6528	0.7954
DenseNet121	0.1553	0.3381	0.6193	0.7906

Table 3. Compare the prediction accuracy and label flip rate of $W \cdot x$ and b with original accuracy of cifar100 test dataset over different CNN architectures.

Network	$W \cdot x$	b_{LFR}	b	Accuracy
ResNet18	0.032	0.4227	0.5029	0.7028
ResNet50	0.056	0.3459	0.5889	0.7673
ResNet152	0.0632	0.3031	0.6354	0.7866

Table 4. Compare the prediction accuracy and label flip rate of $W \cdot x$ and b with original accuracy of 10000 samples of ImageNet validation dataset over different CNN architectures.

4. Experiment

The neural network prediction can be represented as a linear matrix multiplication $F(x) = W \cdot x + b$. How do $W \cdot x$ and b impact the decision of the neural network prediction is important to interpreted the decision of the network model. To evaluate the impact of these two terms in a network prediction, we perform experiments on multiple neural network architectures that trained with MNIST, cifar10, cifar100, and Imagenet datasets.

4.1. Decompose the Model Prediction

Previous section has mentioned that a prediction is described as $F(X) = W \cdot x + b$. To evaluate the impact of

these two terms, we compare the original prediction accuracy of neural network $F(x)$ with the prediction of $W \cdot x$ and b . During the experiment, we use label flip rate (LFR) to track the prediction difference between the select term and the original prediction. The label flip rate is defined as the number of prediction change during the decision process. A smaller LFR value indicates a similar prediction result with the original model. In the experiment, we use stochastic gradient decent(SGD) to train the neural network model. For the MNIST dataset, each model is trained with 50 epochs. The neural network models used for cifar10 and cifar100 are trained with 200 epochs. We use the pre-train models from Pytorch to evaluate the ImageNet dataset.

LeNet300 and LeNet5 are the classical models that used to train MNIST dataset. Both models are trained without batch normalization layer. In Table 1, we compare two models' prediction results with b and $W \cdot x$. The $W \cdot x$ is model accuracy without bias term and $W \cdot x_{LFR}$ is the label flip rate compared with *accuracy* which is the original accuracy of the model. From the evaluation result, we can tell that after removing the bias term, the label flip rates $W \cdot x_{LFR}$ are 0.0082 and 0.0012. The $W \cdot x$ accuracy and original accuracy is similar. In the other hand, the impact of b is an insignificant part of the prediction and the b_{LFR} is large.

However, the observation from MNIST dataset does not generalize to large models and complex datasets. In cifar10, and cifar100 dataset, we use popular convolution architectures (VGG [32], ResNet [10], and DeseNet [11]) to compare the performance of $W \cdot x$ and b . From the results of Table 2 and Table 4, we can tell that bias term b dominates the prediction behavior of a neural network model. Except the network such as LeNet5 and AlexNet, which have relative large impact in both b and $W \cdot x$, the rest of model shows that b has the dominant impact during the model prediction. Using the information from b can determine the majority prediction of the model. In the other hand, the impact of $W \cdot x$ along is not enough to determine the model prediction.

4.2. Explainability of $W \cdot x$

In previous section, we has discussed that decompose the prediction of neural network into 2 components. In the datasets such as MNIST, $W \cdot x$ has similar prediction accuracy as the original model to explain the model prediction. However, for dataset such as cifar10, cifar100 and ImageNet dataset, it does not show promising accuracy to explain the majority prediction of the neural network model. During the model prediction, $b = \sum_{i=1}^{n-1} (W'_n \dots W'_{i+1} \cdot b_i) + b_n$ plays a significant role to determine the prediction. It worth to notice that the convolution layer of convolution neural network model does not contain the bias term. During the model decomposition, the bias term b

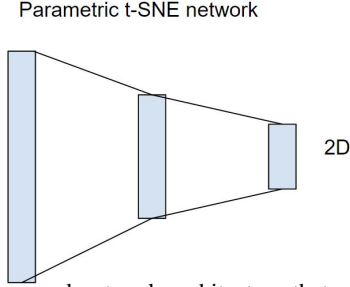


Figure 5. The neural network architecture that used to perform auto encoder training and parametric t-sne dimension reduction.

comes from the batch normalization layers. For each value of b_i , its value is constant and determined once the model is trained. In the equation, the variance that updated is W'_i which is triggered by the activation of the different input. $W = W'_n \cdot W'_{n-1} \dots W'_2 \cdot W'_1$ contains the unique footprint of a model's reaction to a prediction.

An alternative approach to improve the sufficient of W is to train a neural network without batch normalization layer. Since the prediction of these networks can be represented as $F(x) = W \cdot x + b_n$ and b_n is the bias term in the last layer of neural network. We can use the W to explain the network behavior directly. A potential approach to improve the performance of such models include techniques such as weight normalization [24], initialization and other batch normalization free techniques. Previous researches have demonstrate that network training without batch normalization can still achieve state-of-art performance [5]

5. Applications

In this section, we discuss the application of our proposed approach in supervise task, unsupervised task, and ensemble neural network model prediction.

5.1. Supervised Learning - Image Prediction

For MNIST dataset, we use our method to understand the decision of LeNet5, which the encoder layer does not include bias term. The accuracy of the model is 0.9904. For MNIST dataset, W for the final prediction is a (10, 784) matrix and for each digit outcome, W will give an explanation. Each row of W tells how a neural network use input feature to tell the prediction score for that digit. Our feature attribution has natural semantic meaning. The value, which assigned to the input pixel, multiplied with input pixel value is the value of current pixel contribute to the prediction. A positive value has a positive contribution to the prediction and a negative value has a negative contribution.

Figure 6 demonstrates how LeNet5 processes input digits image 1 and 7 for different label decision. In the heat map visualization, the red color indicates the positive contribution and the blue color tells the negative contribution.

From the result, we can tell that both digits are recognized by the neural network model in the right shape. It property of our approach is that compute the our feature attribution, it needs to compute the contribution of input to each neuron in the neural network first. The final feature attribution is a summary of all previous' neuron's contribution. This property brings the convenient to not only understand how neural network use input feature for decision but also provides how each network neuron use input feature to produce activation output. In Figure 7, we display our feature attribution of digits 7 and how top 5 most activate neurons in different layers of LeNet5 use input features.

5.2. Unsupervised Learning - Parametric Dimension Reduction

Dimension reduction such as t-SNE is a popular approach to understand the structure of neural network model. However, the classical t-SNE algorithm is non-parametric. Therefore, how the input is mapped into two dimensional space is unknown. The uninterpretable process of t-SNE dimension reduction cause confusion and misleading during the analysis. Comparing with t-SNE algorithm, parametric t-SNE perform similar operations by training a neural network model to perform the dimension reduction. In this work, we mainly discuss the neural network architecture in Figure 5 to perform the dimension reduction. Many works [37, 35, 14] have developed to implement parametric t-SNE.

The loss function (equation (1)) that used to train parametric t-SNE try to minimize the probability distribution difference between the original high dimension data and the projected low dimension data.

$$L(\theta) = \sum_{i \neq j} p_{ij} \log \frac{p_{ij}}{q_{ij}} \quad (4)$$

$$p_{j|i} = \frac{\exp(-\|x_i - x_j\|^2 / 2\sigma_i^2)}{\sum_{k \neq i} \exp(-\|x_i - x_k\|^2 / 2\sigma_i^2)} \quad (5)$$

$$p_{ij} = \frac{p_{j|i} + p_{i|j}}{2N} \quad (6)$$

$$q_{ij} = \frac{\exp(-\|f_\theta(x_i) - f_\theta(x_j)\|^2 / 2\sigma_i^2)}{\sum_{k \neq i} \exp(-\|f_\theta(x_i) - f_\theta(x_k)\|^2 / 2\sigma_i^2)} \quad (7)$$

Because of the non-linear properties of the neural network model. Understanding the relationship between input and output of these networks trained with different loss function is difficult. In the literature, limited work focus on understanding how input contribute to the final two dimension output. Gradient is the common approach to perform feature attribution of the neural network model. However, it is difficult to generate gradient for a single sample with

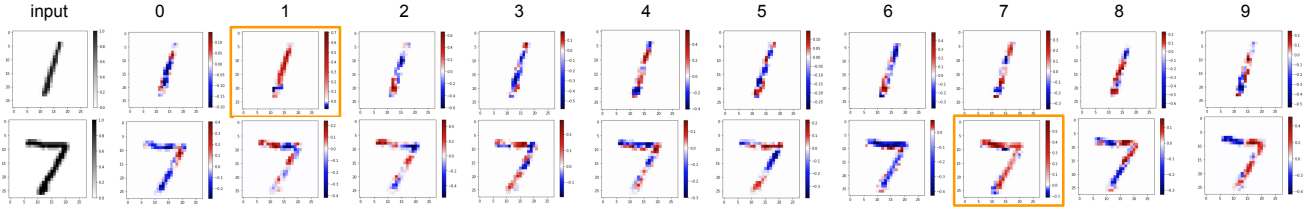


Figure 6. How neural network use input features to make a prediction in MNIST dataset with LeNet5.

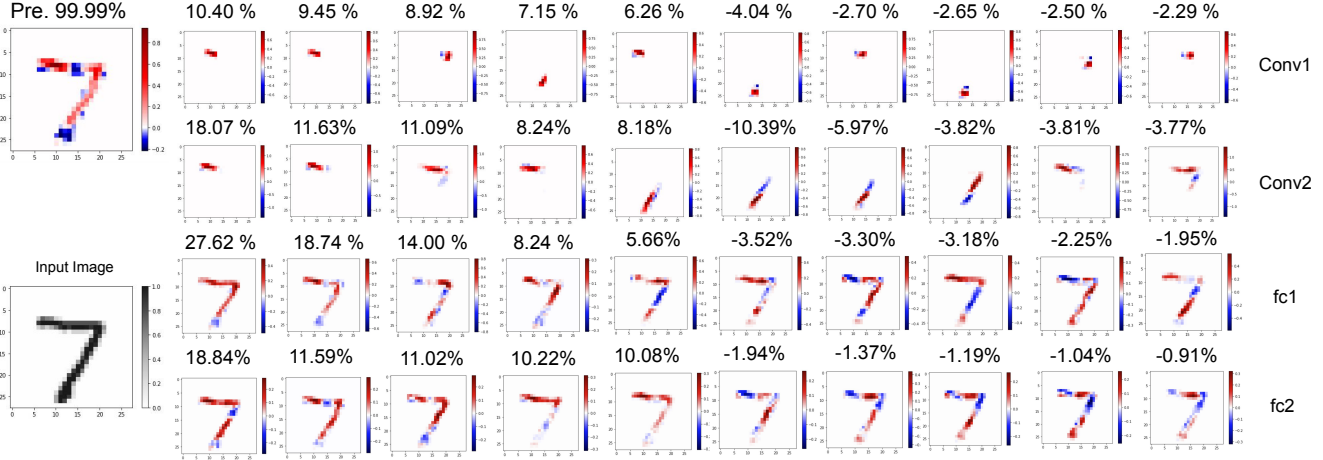


Figure 7. Displaying the features that captured by top 5 positive neurons and 5 negative neurons with their contribution to a model’s final prediction in different layers of the LeNet5 model.

the loss function that used to train neural network for parametric t-SNE. Furthermore, parametric t-SNE [37] may use neural network with an encoder with unsupervised approach to pretrain a network model, then use the neural network to perform the dimension reduction. The overall process involve two neural network model which make the interpretability of the parametric t-SNE difficult. Our approach is flexible enough to fill this gap by concatenate two network’s matrix multiplication to understand the process of the parametric dimension reduction and the final projection can still be phased as $y = Wx + b$ for each sample’s behavior.

What features are used during dimension reduction process is important to interpret the dimension reduction result. In Fig. 8, we apply parametric t-SNE dimension reduction approach on iris dataset and use our proposed method to generate the feature attribution for dimension reduction result. t-SNE dimension reduction often projects samples that are similar to each other to the nearby location. From visualization, samples include (d), (e), (f) are nearby and the feature attribution result over these samples are similar. However, samples (a), (b), (c) are nearby with very different feature attribution result.

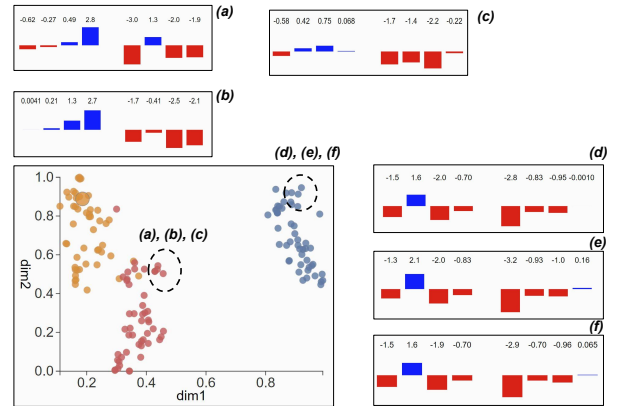


Figure 8. iris flower dataset is projected into two dimensional space with parametric t-SNE. With our feature attribution, it highlights the critical features that are used for dimension reduction.

6. Conclusion

In this work, we propose an approach to reformulating the forward propagation computation to understand a neural network prediction. Our study find that a prediction of neural network can be rephrased as a series of matrix multiplication. For each input instance, its output have a straight forward mapping which can be phrased as $y = W \cdot x + b$. At the end, we demonstrate the flexibility of our approach on

how this approach can help use to understand the supervise classification task, and unsupervised dimension reduction task.

Acknowledgement

Utah funding support, This work was performed under the auspices of the U.S. Department of Energy by Lawrence Livermore National Laboratory under Contract DE-AC52-07NA27344. The work is partially supported by Laboratory Directed Research and Development Program under tracking code 23-ERD-029.

References

- [1] Blueprint for an ai bill of rights, Oct 2022. **1**
- [2] Nongnuch Artrith, Keith T Butler, François-Xavier Coudert, Seungwu Han, Olexandr Isayev, Anubhav Jain, and Aron Walsh. Best practices in machine learning for chemistry. *Nature chemistry*, 13(6):505–508, 2021. **1**
- [3] Sebastian Bach, Alexander Binder, Grégoire Montavon, Frederick Klauschen, Klaus-Robert Müller, and Wojciech Samek. On pixel-wise explanations for non-linear classifier decisions by layer-wise relevance propagation. *PloS one*, 10(7):e0130140, 2015. **2**
- [4] David Bau, Bolei Zhou, Aditya Khosla, Aude Oliva, and Antonio Torralba. Network dissection: Quantifying interpretability of deep visual representations. In *Proceedings of the IEEE conference on computer vision and pattern recognition*, pages 6541–6549, 2017. **2**
- [5] Andy Brock, Soham De, Samuel L Smith, and Karen Simonyan. High-performance large-scale image recognition without normalization. In *International Conference on Machine Learning*, pages 1059–1071. PMLR, 2021. **6**
- [6] Andre Esteva, Brett Kuprel, Roberto A Novoa, Justin Ko, Susan M Swetter, Helen M Blau, and Sebastian Thrun. Dermatologist-level classification of skin cancer with deep neural networks. *nature*, 542(7639):115–118, 2017. **1**
- [7] Ruth Fong, Mandela Patrick, and Andrea Vedaldi. Understanding deep networks via extremal perturbations and smooth masks. In *Proceedings of the IEEE/CVF international conference on computer vision*, pages 2950–2958, 2019. **2**
- [8] Ruth C Fong and Andrea Vedaldi. Interpretable explanations of black boxes by meaningful perturbation. In *Proceedings of the IEEE international conference on computer vision*, pages 3429–3437, 2017. **2**
- [9] Boris Hanin and David Rolnick. Complexity of linear regions in deep networks. In *International Conference on Machine Learning*, pages 2596–2604. PMLR, 2019. **2**
- [10] Kaiming He, Xiangyu Zhang, Shaoqing Ren, and Jian Sun. Deep residual learning for image recognition. In *Proceedings of the IEEE conference on computer vision and pattern recognition*, pages 770–778, 2016. **4, 5**
- [11] Gao Huang, Zhuang Liu, Laurens Van Der Maaten, and Kilian Q Weinberger. Densely connected convolutional networks. In *Proceedings of the IEEE conference on computer vision and pattern recognition*, pages 4700–4708, 2017. **5**
- [12] Sergey Ioffe and Christian Szegedy. Batch normalization: Accelerating deep network training by reducing internal covariate shift. In *International conference on machine learning*, pages 448–456. PMLR, 2015. **4**
- [13] John Jumper, Richard Evans, Alexander Pritzel, Tim Green, Michael Figurnov, Olaf Ronneberger, Kathryn Tunyasuvunakool, Russ Bates, Augustin Žídek, Anna Potapenko, et al. Highly accurate protein structure prediction with alphafold. *Nature*, 596(7873):583–589, 2021. **1**
- [14] Chien-Hsun Lai, Ming-Feng Kuo, Yun-Hsuan Lien, Kuan-An Su, and Yu-Shuen Wang. Parametric dimension reduction by preserving local structure. In *2022 IEEE Visualization and Visual Analytics (VIS)*, pages 75–79, 2022. **6**
- [15] Guang-He Lee, David Alvarez-Melis, and Tommi S Jaakkola. Towards robust, locally linear deep networks. *arXiv preprint arXiv:1907.03207*, 2019. **2**
- [16] Scott M Lundberg and Su-In Lee. A unified approach to interpreting model predictions. *Advances in neural information processing systems*, 30, 2017. **1, 2**
- [17] Guido F Montufar, Razvan Pascanu, Kyunghyun Cho, and Yoshua Bengio. On the number of linear regions of deep neural networks. *Advances in neural information processing systems*, 27, 2014. **2, 4**
- [18] Roman Novak, Yasaman Bahri, Daniel A Abolafia, Jeffrey Pennington, and Jascha Sohl-Dickstein. Sensitivity and generalization in neural networks: an empirical study. *arXiv preprint arXiv:1802.08760*, 2018. **2**
- [19] Chris Olah, Alexander Mordvintsev, and Ludwig Schubert. Feature visualization. *Distill*, 2(11):e7, 2017. **2**
- [20] Vitali Petsiuk, Abir Das, and Kate Saenko. Rise: Randomized input sampling for explanation of black-box models. *arXiv preprint arXiv:1806.07421*, 2018. **2**
- [21] Maithra Raghu, Ben Poole, Jon Kleinberg, Surya Ganguli, and Jascha Sohl-Dickstein. On the expressive power of deep neural networks. In *international conference on machine learning*, pages 2847–2854. PMLR, 2017. **2**
- [22] Marco Tulio Ribeiro, Sameer Singh, and Carlos Guestrin. ” why should i trust you?” explaining the predictions of any classifier. In *Proceedings of the 22nd ACM SIGKDD international conference on knowledge discovery and data mining*, pages 1135–1144, 2016. **1, 2**
- [23] Haakon Robinson, Adil Rasheed, and Omer San. Dissecting deep neural networks. *arXiv preprint arXiv:1910.03879*, 2019. **2**
- [24] Tim Salimans and Diederik P. Kingma. Weight normalization: A simple reparameterization to accelerate training of deep neural networks. In *Proceedings of the 30th International Conference on Neural Information Processing Systems, NIPS’16*, page 901–909, Red Hook, NY, USA, 2016. Curran Associates Inc. **6**
- [25] Ramprasaath R Selvaraju, Michael Cogswell, Abhishek Das, Ramakrishna Vedantam, Devi Parikh, and Dhruv Batra. Grad-cam: Visual explanations from deep networks via gradient-based localization. In *Proceedings of the IEEE international conference on computer vision*, pages 618–626, 2017. **2**
- [26] Andrew W Senior, Richard Evans, John Jumper, James Kirkpatrick, Laurent Sifre, Tim Green, Chongli Qin, Augustin

- Židek, Alexander WR Nelson, Alex Bridgland, et al. Improved protein structure prediction using potentials from deep learning. *Nature*, 577(7792):706–710, 2020. 1
- [27] Thiago Serra and Srikumar Ramalingam. Empirical bounds on linear regions of deep rectifier networks. In *Proceedings of the AAAI Conference on Artificial Intelligence*, volume 34, pages 5628–5635, 2020. 2
- [28] Thiago Serra, Christian Tjandraatmadja, and Srikumar Ramalingam. Bounding and counting linear regions of deep neural networks. In *International Conference on Machine Learning*, pages 4558–4566. PMLR, 2018. 2
- [29] Avanti Shrikumar, Peyton Greenside, and Anshul Kundaje. Learning important features through propagating activation differences. In *International conference on machine learning*, pages 3145–3153. PMLR, 2017. 2
- [30] David Silver, Aja Huang, Chris J Maddison, Arthur Guez, Laurent Sifre, George Van Den Driessche, Julian Schrittwieser, Ioannis Antonoglou, Veda Panneershelvam, Marc Lanctot, et al. Mastering the game of go with deep neural networks and tree search. *nature*, 529(7587):484–489, 2016. 1
- [31] Karen Simonyan, Andrea Vedaldi, and Andrew Zisserman. Deep inside convolutional networks: Visualising image classification models and saliency maps. *arXiv preprint arXiv:1312.6034*, 2013. 2
- [32] Karen Simonyan and Andrew Zisserman. Very deep convolutional networks for large-scale image recognition. *arXiv preprint arXiv:1409.1556*, 2014. 5
- [33] Daniel Smilkov, Nikhil Thorat, Been Kim, Fernanda Viégas, and Martin Wattenberg. Smoothgrad: removing noise by adding noise. *arXiv preprint arXiv:1706.03825*, 2017. 2
- [34] Mukund Sundararajan, Ankur Taly, and Qiqi Yan. Axiomatic attribution for deep networks. In *International conference on machine learning*, pages 3319–3328. PMLR, 2017. 2
- [35] Mats Svantesson, Håkan Olausson, Anders Eklund, and Magnus Thordstein. Get a new perspective on eeg: Convolutional neural network encoders for parametric t-sne. *Brain Sciences*, 13(3):453, 2023. 6
- [36] Jessica Vamathevan, Dominic Clark, Paul Czodrowski, Ian Dunham, Edgardo Ferran, George Lee, Bin Li, Anant Madabhushi, Parantu Shah, Michaela Spitzer, et al. Applications of machine learning in drug discovery and development. *Nature reviews Drug discovery*, 18(6):463–477, 2019. 1
- [37] Laurens Van Der Maaten. Learning a parametric embedding by preserving local structure. In *Artificial intelligence and statistics*, pages 384–391. PMLR, 2009. 6, 7
- [38] Michael Veale and Frederik Zuiderveen Borgesius. Demystifying the draft eu artificial intelligence act—analysing the good, the bad, and the unclear elements of the proposed approach. *Computer Law Review International*, 22(4):97–112, 2021. 1
- [39] Matthew D Zeiler and Rob Fergus. Visualizing and understanding convolutional networks. In *European conference on computer vision*, pages 818–833. Springer, 2014. 2
- [40] Bolei Zhou, Aditya Khosla, Agata Lapedriza, Aude Oliva, and Antonio Torralba. Object detectors emerge in deep scene cnns. *arXiv preprint arXiv:1412.6856*, 2014. 2
- [41] Yilun Zhou, Serena Booth, Marco Tulio Ribeiro, and Julie Shah. Do feature attribution methods correctly attribute features? In *Proceedings of the AAAI Conference on Artificial Intelligence*, volume 36, pages 9623–9633, 2022. 1